U-Pb zircon (ID-TIMS and SHRIMP) evidence for the early ordovician intrusion of metagranites in the late Proterozoic Canaveilles Group of the Pyrenees and the Montagne Noire (France)

Alain Cocherie, Thierry Baudin, Albert Autran, Catherine Guerrot, C. Mark Fanning, Bernard Laumonier

Bull. Soc. géol. Fr., 2005, t. 176, n° 3, pp. 269-282

U-Pb zircon (ID-TIMS and SHRIMP) evidence for the early ordovician intrusion of metagranites in the late Proterozoic Canaveilles Group of the Pyrenees and the Montagne Noire (France)

ALAIN COCHERIE[1], THIERRY BAUDIN[1], ALBERT AUTRAN[2], CATHERINE GUERROT[1], C. MARK FANNING[3] and BERNARD LAUMONIER[4]

Key words. – Ordovician, Precambrian, U-Pb dating, Zircon, Orthogneiss, Metavolcanite, Pyrenees, Montagne Noire

Abstract. – Depending on the quality of the zircon grains available for analysis, two methods may be used to date igneous rock emplacement, namely U-Pb TIMS with isotope dilution or *in situ* U-Pb SIMS (SHRIMP). Both methods have been used to determine, in a precise and accurate manner, the emplacement age of the granitic protolith of the various orthogneisses in the Pyrenean Axial Zone. More specifically, four representative samples of G1, G2 and a "transition gneiss" yielded reliable datings with an average age of 473 ± 4 Ma for each sample. The surrounding sediments of the Canaveilles Group were constrained by zircon grains from interlayered metarhyodacite and dated at 581 ± 10 Ma using the SHRIMP method, clearly giving this group a late Proterozoic (Vendian) age. Finally, the Somail orthogneiss of the Montagne Noire, equivalent to that of the Canigou, yielded an age of 471 ± 4 Ma with the *in situ* U-Pb method, which is identical to the dating of the Pyrenean samples. In addition, most of the studied orthogneisses recorded a wide range of significant concordant inherited ages spanning from early Archaean (3.5 Ga) to Pan-African/Cadomian (600-800 Ma). Bearing in mind the calc-alkaline affinity of the studied rocks, this work demonstrates the huge contrast between the active Gondwana margin in the north ("South European terrane") and the remarkably homogeneous continental plate that existed from Arabia to Morocco during the Ordovician.

Age ordovicien inférieur pour l'intrusion des méta-granites dans le groupe protérozoïque terminal de Canaveilles dans les Pyrénées et la Montagne Noire (France) : U-Pb sur zircon (dilution isotopique et SHRIMP)

Mots clés. – Ordovicien, Précambrien, datation U-Pb, Zircon, Orthogneiss, Métavolcanites, Pyrénées, Montagne Noire

Résumé. – En fonction de la qualité des zircons disponibles et de la nature du problème géochronologique à résoudre, deux méthodes U-Pb sur zircon peuvent être envisagées pour dater la cristallisation d'une roche magmatique: soit la méthode U-Pb par dilution isotopique, après dissolution des grains et analyse par TIMS (spectrométrie de masse par thermo-ionisation), soit par l'analyse U-Pb *in-situ* à l'aide d'une microsonde ionique de haute résolution (SHRIMP). Ces deux méthodes sont apparues indispensables pour dater sans ambiguïté la mise en place des protolithes granitiques de divers orthogneiss de la zone axiale des Pyrénées, longtemps considérés, par certains auteurs, comme un « socle cadomien ». Ainsi, quatre échantillons représentatifs des gneiss G1, G2 et de transition ont été datés. Des âges identiques dans la limite des erreurs à ± 2 σ, précis et fiables, ont été obtenus: deux gneiss de type G1-La Preste à 477 ± 4 et 472 ± 6 Ma, un gneiss G2 à 471 ± 8 Ma et un gneiss de transition à 467 ± 7 Ma. Ces datations démontrent un âge moyen de 473 ± 4 Ma (fin de l'Ordovicien inférieur) pour la mise en place des protolithes, si on tient compte de l'âge à 475 ± 10 Ma obtenu par Deloule *et al.* [2002] sur une combinaison des faciès G1 et G2. Par ailleurs, une méta-rhyodacite, interstratifiée près de la base du Groupe de Canaveilles, a été datée du Vendien à 581 ± 10 Ma (SHRIMP) permettant ainsi d'assigner un âge anté-ordovicien à la sédimentation. Enfin, des orthogneiss équivalents à ceux du Canigou sont connus dans la Montagne Noire sous le nom d'orthogneiss de Somail. La datation *in situ* des zircons d'un orthogneiss de ce type, prélevé au col de Cabaretou a permis de calculer un âge identique à ceux des Pyrénées à 471 ± 4 Ma. La plupart de ces orthogneiss ont dû être datés à l'aide d'une sonde ionique afin de pallier aux phénomènes d'héritage dont il est souvent difficile de s'affranchir par dilution isotopique après dissolution (ID-TIMS).

Ce faisant, un large éventail d'âges hérités concordants a été mis en évidence depuis le Pan Africain / Cadomien (600-800 Ma), jusqu'à l'Archéen précoce (2,8 et même 3,5 Ga) en passant par le méso-Protérozoïque (1016, 1033 et 1046 Ma), le paléo-Protérozoïque (2009 Ma) et l'Archéen terminal (2,5 Ga).

Entre l'Ordovicien inférieur et moyen, l'intense activité magmatique et les variations sédimentologiques qui caractérisent l'ensemble des terrains sud-européens (Massif armoricain, Massif central, Alpes, Ibérie, Pyrénées et Montagne Noire) plaident en faveur d'une « individualisation » de ces terrains par rapport à la marge gondwanienne. En effet, cette dernière se distingue particulièrement au cours de l'Ordovicien par la persistance d'une plate-forme continentale terrigène remarquablement homogène qui se suit depuis l'Arabie jusque dans l'Anti-Atlas marocain. Il faut donc envisager dès l'Ordovicien, le morcellement et la séparation des blocs sud-européens de la marge passive nord-gondwanienne.

[1] BRGM, BP 6009, 45060 Orléans cedex 2, France (a.cocherie@brgm.fr).
[2] 15 rue Nicolas Poussin, 45100 Orléans, France.
[3] Research School of Earth Sciences, ANU, Canberra, ACT 0200, Australia.
[4] LAEGO – Mines, Ecole des Mines, 54502 Vandœuvre-les-Nancy cedex, France.
Manuscrit déposé le 29 juin 2004; accepté après révision le 6 janvier 2005.

Le chimisme calco-alcalin à alumineux des orthogneiss des Pyrénées et de la Montagne Noire, de par la rareté des faciès basiques à tonalitiques, n'apporte pas d'indication décisive sur le contexte géodynamique de leur mise en place. Par contre, la typologie de leurs zircons de type « anatexie crustale – S » et/ou « calco-alcaline – I » ainsi que les faciès de type « rapakivi » assez répandus, symptomatiques de cristallisation par mélange de magmas en déséquilibre, suggèrent leur formation par fusion crustale (S) et subcrustale (I) étagée dans un environnement thermique anormalement élevé. Ce magmatisme évolue à la fin de l'Ordovicien ou au Silurien (dans le massif Catalan) vers des basaltes alcalins (Dôme de Pierrefitte dans les Pyrénées centrales) ou des granites à tendance alcaline dont les Gneiss de Casemi dans le massif du Canigou [datés à 425 ± 8 Ma par Delaperrière et Soliva, 1992] sont un exemple.

Dans les Pyrénées et la Montagne Noire, la discordance de l'Ordovicien supérieur sur le Cambrien signale l'existence d'une déformation modérée et d'une émersion que l'on pourrait rattacher à une cordillère distensive émergée. C'est dans une telle intumescence thermique qu'on pourrait envisager l'origine du plutonisme ordovicien des Pyrénées et de la Montagne Noire. Un exemple plus récent de cette sorte de magmatisme peut être observé dans les granites tertiaires et les volcans qui intrudent la croûte continentale du plateau du Colorado, à l'est de la zone de rift du « Basin and Range », très loin de la fosse de subduction occidentale.

INTRODUCTION

The eastern part of the Pyrenean Axial Zone is characterised by the existence of orthogneiss massifs whose age and geodynamic significance have had a major impact on the understanding of the pre-Variscan evolution of this region. The orthogneisses (Aston, Hospitalet, Canigou, Roc de France and Albères) occupy the deeper parts of the Axial Zone, and it is mainly due to the interpretation of their upper contact with the overlying metasediments (Canaveilles Group) that they have been considered as constituents of a Cadomian basement [Autran *et al*., 1966; Laumonier and Guitard, 1986].

Indeed, the remarkable parallelism of the top of the orthogneisses and the metasediments, which can be mapped over several tens of kilometres, initially led authors to take this as a major argument for a basement-cover relationship [Autran *et al*., 1966; Guitard *et al*., 1996], characterised by a transgression of the sedimentary successions younging towards the west [Laumonier, 1998].

Backed up by these field data, a model of the orthogneissic Cadomian basement was built on the basis of U-Pb dating (dissolution on large fractions of zircon populations) at 580 ± 20 Ma [Vitrac-Michard and Allègre, 1975b]. This U-Pb age, which is not precise, has prevailed over Rb-Sr ages that yielded ages of ~475 Ma for the Ordovician [Jäger and Zwart, 1968] and ~524 Ma for the Cambrian [Vitrac-Michard and Allègre, 1975a]. More recently, further Ordovician ages for these orthogneisses were determined for a metaleucogranite in the Aston massif by Majoor [1988]. In addition, three facies of the Canigou massif already indicated an Ordovician age for these orthogneisses [Cocherie *et al*., 1992; Guitard *et al*., 1996; Delaperrière and Respaut, 1995], despite being considered questionable at the time (Pb-evaporation method). Renewed detailed mapping and structural interpretation, gave rise to new U-Pb datings confirming an Ordovician age for the orthogneisses of the Canigou [Deloule *et al.,* 2002], but also in the Montagne Noire [Roger *et al.,* 2004]. The five new ages presented here allow us to give the same Ordovician age to all the different granitic facies of the orthogneisses in the Pyrenees and the Montagne Noire (fig. 1).

However, the acceptance of this Ordovician age does not directly call into question the notion of a basement-cover relationship, so ardently defended in the past. Indeed, it would be conceivable to consider that the azoic cover (Canaveilles Group) is middle to late Ordovician in age, as proposed by Konzalova *et al.* [1982]. The intrusion features observed in some localities at the base of the orthogneisses [Guitard *et al.,* 1996] have been interpreted as also pertaining to an older basement.

Despite the strong presumption of a terminal Precambrian to early Ordovician age [Laumonier, 1988, 1996, 1998; Barbey *et al.,* 2001], on the basis of a facies comparison with the neighbouring regions, the controversy regarding the age of the azoic Canaveilles Group (above and beneath the orthogneisses bodies) necessitated precise geochronological data.

To achieve these aims, we chose to adopt the *in situ* U-Pb zircon ion microprobe method (SHRIMP) for four of the six datings in order to take into account the problem raised by contribution from the inherited zircons common in these orthogneisses. It was also necessary to demonstrate that the range of facies represented by the orthogneisses of the Canigou – Roc de France indeed belonged to a single magmatic episode. In fact, among the two published datings relating to these orthogneisses, the first [Delaperrière and Respaut, 1995] only dealt with the latest and most acid facies (Type G1-La Preste), and the second [Deloule *et al.,* 2002] constituted a composite age for four zircons from three samples representing two different facies. Furthermore, we also wanted to confirm, using the same geochronological method, the recognised lithological analogies between the axial zone of the Pyrenees and that of the Montagne Noire [Laumonier, 1988; Demange, 2003; Clausen and Alvaro, 2004; Roger *et al.,* 2004] by dating, at the latter location, the Somail orthogneiss in its part least affected by metamorphism. Finally, the concordant inherited ages provide important information on the ancient history of the continental crust in this external sector of the Hercynian chain.

GEOLOGICAL CONTEXT AND SAMPLE LOCATION

During the Carboniferous, the Hercynian orogeny affected the Palaeozoic and older formations of the eastern part of the Pyrenean Axial Zone. The whole area was affected by HT-LP metamorphism, and was immediately accompanied by intrusion of the late Carboniferous granites. Despite the imprint of Alpine and Hercynian tectonism, the structural organisation of the eastern part of the Axial Zone can be described by three successions. These are, from the bottom upwards:

– huge orthogneiss bodies (up to 3000 m thick) intruding mica schist or intensely metamorphosed, even anatectic paragneisses. These orthogneisses derive from the porphyritic monzonitic granites that constitute the main facies of the massifs of the Canigou, the Roc de France, the Aston and the Hospitalet;

– overlying the orthogneiss is a thick (~5000 m) fine-grained terrigenous azoic succession with carbonate and volcanic layers, which is subdivided into the lower Canaveilles Group and the upper Jujols Group [Cavet, 1957; Laumonier, 1988]. Until now, the age of this succession has remained a subject of controversy, believed to be either Ordovician [Konzalova *et al.*, 1982] or, the more probable option, late Proterozoic to Cambrian [Laumonier, 1998];

– a transgressive succession showing cartographic uncomformity, starting in the late Ordovician and ending with the synorogenic flysch of the late Carboniferous.

The orthogneisses of the Canigou-Roc de France have been classified into three gneiss facies [Guitard, 1970] according to their decreasing quartz and increasing biotite contents: G1 (peraluminous granite), G2 (biotite-bearing monzogranite) and G3 (biotite granodiorite). The facies can be isogranular or contain K-feldspar phenocrysts, commonly with rapakivi textures. Similar facies types are also found in the orthogneisses of the massifs of the Albères, the Aston and the Hospitalet. The G1 facies is subdivided into two types: G1-La Preste and G1-Carança, the former being distinguished from the latter in the field by the presence of blue-tinged quartz phenocrysts and microgranular facies. The various facies grade progressively from one to another, G3 being located at the base and in the central zone of the laccolith, whereas G1 is located at its summit and edge. A G1-type satellite orthogneiss body, associated with isogranular leucogranite, is separated from the main unit and forms a thin laccolith interstratified at the base of the Canaveilles succession stretching several tens of kilometres to the south (Nuria) and the west of the Massif de Carança. This reference level (Queralbs or Bassibès), sometimes interpreted as being volcanic or arkosic in origin [Guitard, 1970; Laumonier, 1988 and 1998], in fact represents a gneissified granitic sill (transition gneiss), as has already been envisaged by Guitard *et al.* [1996].

Four new datings were carried out on the Canigou – Roc de France massif and concern two G1-La-Preste-type samples (LP1 and LP2), a G2-Rapakivi-type sample (CAN2), and a transition gneiss from the Bassibès sill (BAS 1) in order to verify that it belongs to the Canigou magmatic suite (fig. 1 and table I). The azoic Canaveilles Group, which needed to be geochronologically dated, comprises in its median member the interstratified metavolcanics descri-

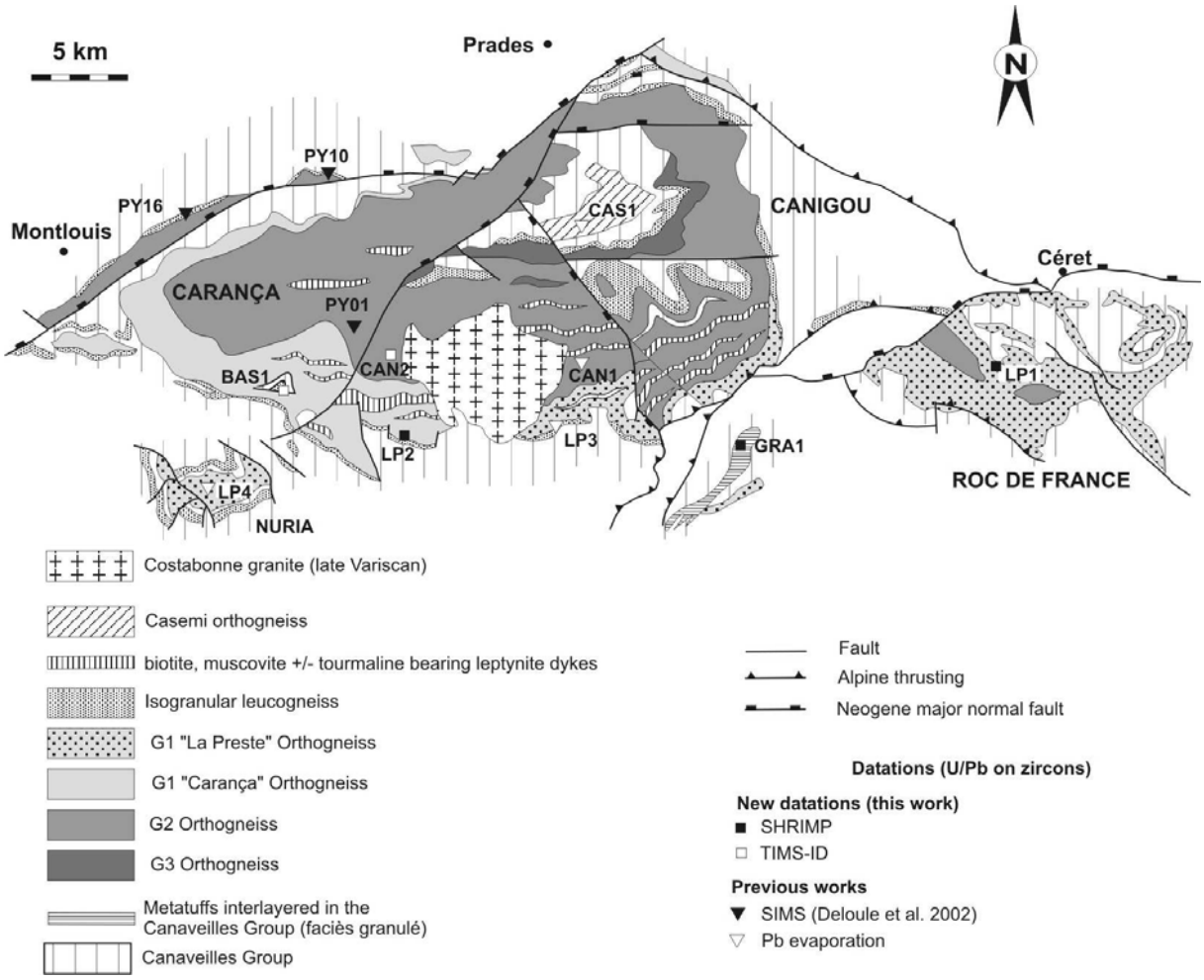

FIG. 1. – Simplified geological map of the study area in the Pyrenees (France).
FIG. 1. – *Carte géologique simplifiée de la zone étudiée des Pyrénées (France).*

TABLE I. – Summary of studied samples and previous studies for similar orthogneiss.
TABL. I. – *Synthèse des données obtenues dans ce travail et par des travaux antérieurs sur des orthogneiss similaires.*

Sample #	Rock type	Age (Ma)	Sampling site	X	Y
CAN2	G2	471 ± 8 (U-Pb TIMS ID)	Rocs Blancs, Wof Mantet pass	597178	1714643
BAS1	Transition gneiss	467 ± 7 (U-Pb TIMS ID)	Pass, south of Peak of Prats de Bassibès (Carança)	591338	1714168
LP1	G1-LA PRESTE	477 ± 4 (U-Pb SHRIMP)	D53 road, Montalba,Can Riubanys	628058	1716278
LP2	G1-LA PRESTE	472 ± 6 (U-Pb SHRIMP)	Track (South of Roc Colom), del Forquets torrent	598376	1711775
SOM 1	Somail orthogneiss	471 ± 4 (U-Pb SHRIMP)	Montagne Noire, D607 road, 2 Km W Caberetou pass	2°44'45"	45°30'12"
GRA1	"Sitges" lapillis	581 ± 10 (U-Pb SHRIMP)	D115 road, left bank of Tech river, St. Eloi oratory	615440	1711444
CAN1 (1)	G2	451 ± 14 (Pb-evaporation)	Collade Grande, Pla Guillem road	607009	1715035
LP3 (2)	G1-LA PRESTE	446 ± 20 (Pb-evaporation)	North La Preste, forest road: Torres d'En Preste	607203	1713152
LP4 (3)	G1-LA PRESTE	461 ± 7 (Pb-evaporation) 570 ± 9 (Pb-evaporation)	Nuria - Torrente de la Bauma (1350 m)		
CAS1 (4)	Orthogneiss Casemi	425 ± 18 (Pb-evaporation)	200 m North Marialles hut	605850	1722000
PY01 (5)	G2		Caret crest, GR10 path (Carança)	594609	1717076
PY10 (5)	G1	475 ± 10 (U-Pb IMS 1270)	Les Graus - Thuès les Bains		
PY16 (5)	G1		Llar road - Fontpédrouse		

(1) Cocherie [1992], *in* Guitard *et al.* [1996]
(2) Delaperrière & Respaut [1955]
(3) Calvez [1990] *in* Guitard *et al.* [1996]
(4) Delaperrière & Soliva [1922]
(5) Deloule *et al.* [2002]

bed by Guitard [1970] as the so-called "*faciès granulés*", which are derived from homogeneous "lapillitic" rhyodacites. This is the thickest level (200 m) that enabled dating (GRA 1). The final dating was performed on a lateral equivalent of the Canigou orthogneiss in the Montagne Noire, namely the Somail orthogneiss (SOM 1).

U-Pb GEOCHRONOLOGY

Analytical procedures

All of the datings during the course of this study were obtained using the U-Pb zircon method. However, two analytical approaches were used depending on the quality of the available minerals. The conventional approach, involving zircon dissolution and known as ID-TIMS, is very precise and allows highly sensitive correction of common Pb. It can be applied to batches of three to six zircons, even single grains, when the size and the age range permit. The method is very suitable for zircons lacking inherited cores and with a transparent appearance. The other approach, the *in situ* ion microprobe or SHRIMP, makes it possible to analyse uniquely the fresh areas of altered grains or to select the core or the edge of grains with a complex history. After a classical separation of heavy minerals for the ID-TIMS method, the zircons were separated according to their magnetic susceptibility, the least magnetic often being the most concordant [e.g. Krogh, 1982a]. They were then divided into distinct morphological populations and highly abraded in order to improve concordancy [Krogh, 1982b]. Grains with inherited cores were carefully avoided since ID-TIMS analytical results for polygenetic zircons are not easy to interpret. The processes for dissolution of the zircon fractions and separation and purification of uranium and lead were adapted from Krogh [1973] and Parrish [1987]. The analyses were carried out in dynamic mode with an electron multiplier using a Finnigan MAT 261 (BRGM) mass spectrometer. The contamination levels were less than 15 pg for Pb and 1 pg for U. The measured ratios were corrected for mass fractionation, procedural blank, spike contribution, and initial common lead using the model described by Stacey and Kramers [1975] (see table II).

The ion microprobe analyses were carried out on the SHRIMP II of the Australian National University in Canberra, according to the procedure described by Williams [1998]. The areas analysed were selected after studying images of the grains obtained by cathodoluminescence and by transmitted-light microphotography. The determination of the $^{238}U/^{206}Pb$ ratio necessitated the external calibration of the measurements with the aid of a particularly homogeneous standard zircon of known isotope composition: the Duluth Gabbro [Paces and Miller, 1993]. In general, areas very rich in U (> 2000 ppm) were not selected in order to avoid, firstly, moving away from the area of validity of the U-Pb calibration line and, secondly, the risk of losses of radiogenic Pb, in relation to the metamictisation. For the relatively recent zircons (< 1000 Ma), the analytical uncertainty of the $^{206}Pb/^{204}Pb$ ratio becomes critical; one then uses the Concordia diagram of Tera and Wasserburg [1972], modified by Compston *et al.* [1992], where one plots the $^{207}Pb/^{206}Pb$ and $^{238}U/^{206}Pb$ ratios, not corrected for common Pb. In the absence of common Pb, the analyses of areas not affected by thermal events subsequent to the crystallisation of the zircon or by inherited cores plot along this Concordia [Williams, 1998]. Although the variable quantities of common Pb adversely affect the values of the two ratios, these data points form a straight line passing through the composition of common Pb ($^{207}Pb/^{206}Pb$) at the estimated age of the system given, in a first approximation, by the average $^{238}U/^{206}Pb$ ages stemming from the concordant analyses. The extrapolation of this line on the Concordia defines the sought age. This procedure is called common Pb correction by the ^{207}Pb method as opposed to the ^{204}Pb method, as in the case of the conventional diagram. Using this correction method, one calculates the $^{206}Pb^*/^{238}U$ (Pb* = radiogenic Pb) ratios for each point as well as the related $^{206}Pb^*/^{238}U$ ages listed in table III. Therefore, the calculation of the weighted average age of a selection of $^{206}Pb^*/^{238}U$ ages leads to the same mean age and error as the calculated intercept of the regression line with the Concordia, using the same data.

TABLE II – Conventional U-Pb zircon data for two samples from Pyrénées. Analyses in italic were not considered for age calculation.
TABL. II. – *Données U-Pb en dissolution sur deux échantillons des Pyrénées. Les analyses en italique ne sont pas considérées dans le calcul de l'âge.*

Sample	Concentrations				Isotopic ratios					Age
	Wt. (µg)	U (ppm)	Pb rad. (ppm)	Pb com. (pg)	$^{206}Pb/^{204}Pb$	$^{208}Pb/^{206}Pb$	$^{206}Pb/^{238}U$	$^{207}Pb/^{235}U$	$^{207}Pb/^{206}Pb$	$^{207}Pb/^{206}Pb$ (Ma)
[1]				[2]	[3]	[4]	[4]	[4]	[4]	
Meta-monzogranite (CAN 2)										
1 5 gr, m1	10	294	20,7	22	623	0,058	0.07346 ± 44	0.5720 ± 44	0.05647 ± 26	471
2 4 gr, m1	*7*	*615*	*44,1*	*18*	*1105*	*0,072*	*0.07371 ± 26*	*0.6112 ± 32*	*0.06014 ± 24*	*609*
3 4 gr, m1	*10*	*448*	*32,0*	*19*	*1096*	*0,065*	*0.07378 ± 30*	*0.6254 ± 38*	*0.06148 ± 30*	*656*
4 5 gr, m1	26	289	20,5	30	1155	0,049	0.07467 ± 28	0.5814 ± 26	0.05648 ± 14	471
5 6 gr, m1	20	501	35,2	27	1683	0,081	0.07173 ± 22	0.5583 ± 22	0.05645 ± 10	470
Meta-leucogranite (BAS 1)										
1 3 gr, m1	*19*	*381*	*26,9*	*16*	*2006*	*0,077*	*0.07231 ± 40*	*0.5864 ± 34*	*0.05881 ± 14*	*560*
2 4 gr, m1	14	288	20,9	33	588	0,068	0.07507 ± 22	0.5835 ± 28	0.05637 ± 20	467
3 4 gr, m1	16	376	26,4	36	754	0,081	0.07175 ± 28	0.5576 ± 28	0.05637 ± 20	467
4 5 gr, m1	23	206	15,2	17	1260	0,116	0.07334 ± 26	0.5698 ± 26	0.05635 ± 14	466
5 6 gr, m1	*21*	*382*	*27,7*	*51*	*755*	*0,056*	*0.07571 ± 40*	*0.6018 ± 38*	*0.05765 ± 18*	*517*

[1] Number of grains; m1: magnetic at 1°
[2] total common Pb (involving isotopic tracer contribution, blank contamination and the mineral itself)
[3] corrected for mass discrimination
[4] corrected for mass discrimination, procedural blank (Pb=15 pg, U=1 pg), isotopic tracer and initial common Pb.
Errors given at the 2σ level, initial common Pb composition according to the stage model of Stacey and Kaners [1975]

Whatever the analytical approach used, all the uncertainty calculations were made at the 2σ level (95% confidence limit) using the ISOPLOT/EX program (version 2.34) of Ludwig [2000]. On the other hand, in the case of the data obtained using the SHRIMP, the uncertainties are given at 1σ in the corresponding tables and, in the same way, the error ellipses are given at 1σ in order to make the figures easier to read. This is in agreement with the whole data from articles involving SHRIMP [e.g. Williams, 2001; Gray *et al.,* 2004].

Metamonzogranite CAN 2

Sample CAN-2 is a biotite-bearing porphyritic metamonzogranite belonging to the G2-type Rapakivi K-feldspar facies. The zircons in this rock are abundant but relatively small. They are pink coloured and generally transparent. Some of the darker zircons are zoned. From a morphological point of view, it was possible to characterise 50% of the crystals. They plot essentially in the central part of the typological distribution diagram of Pupin [1980]. Two populations seem to coexist: (i) a calc-alkaline I-trend population with zircons completely to the right of the diagram (P1-3; G; S5) and in the centre (S14-15 and S25); (ii) a population with clear anatectic crustal S-trend (S3-4; S6-8; S12-13) in the centre and to the left of the diagram (fig. 2b). The results obtained on the five fractions analysed are shown in table II, and on the Concordia diagram in figure 3a. The five fractions were assumed to be similar, as they were all composed of clear zircon grains with low magnetic properties and seemingly without any inheritance. Fractions 1, 4 and 5 are well aligned in the

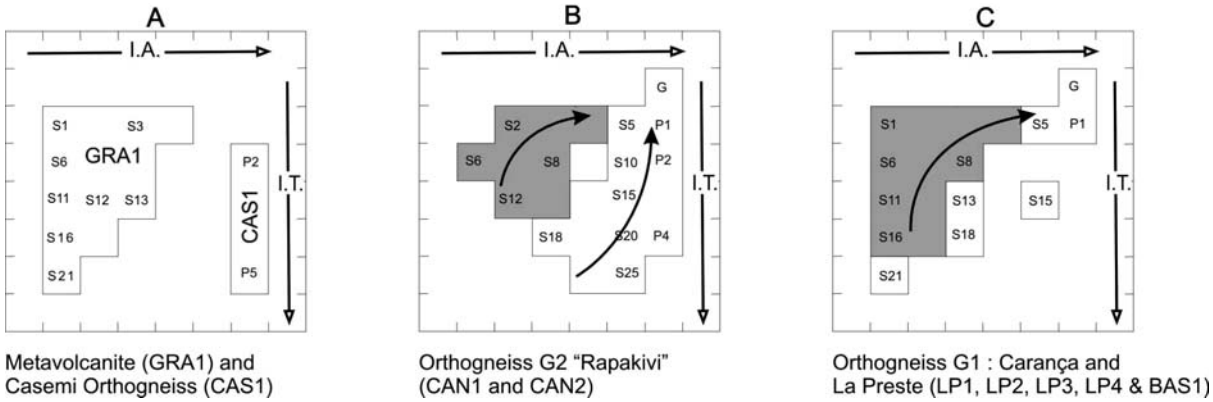

FIG. 2. – Typology of dated zircons [Pupin, 1980]. Grey area: morphology of zircons observed in all of the aluminous metagranites studied and attributed to a crustal anatexis origin (S) with their evolution with decreasing temperature of the magma (black arrows). One observes in B the coexistence of lines I and S in the "Rapakivi" gneiss G2 and on A the exclusively crustal anatexis zircons in the lapilli tuffs of the Neo-Proterozoic (transition gneiss GRA 1), clearly distinct from the hypoaluminous magmas I (CAS 1) of the late Ordovician (separations and morphological analyses carried out by P. Jézéquel – BRGM).
FIG. 2. – *Typologie des zircons datés [Pupin, 1980]. Domaine en grisé : morphologie des zircons observés dans tous les métagranites étudiés : en* C *: granitoïdes alumineux attribués à une origine par anatexie crustale* (S) *avec leur évolution à température décroissante du magma (flèches noires). On remarquera en* B *la coexistence des lignées* I *et* S *dans les gneiss G2 « rapakivi » et sur A les zircons exclusivement d'anatexie crustale dans les tufs à lapillis du Néoproterozoïque (gneiss de transition GRA 1) clairement distincts des magmas hypoalumineux I (CAS1) de l'Ordovicien supérieur (séparations et analyses morphologiques des zircons réalisées par P. Jézéquel – BRGM).*

Concordia diagram with homogeneous $^{207}Pb/^{206}Pb$ ages of 470 Ma, with fraction 4 being subconcordant. However, fractions 2 and 3 indicate the presence of ancient lead, with $^{207}Pb/^{206}Pb$ ages of 610 and 660 Ma. They would indicate a late Proterozoic heritage in agreement with the anatectic nature suggested by a portion of the zircon population. The regression by fractions 1, 4 and 5 defines a Discordia that cuts through the Concordia at 471 ± 8 Ma: (the lower intercept is located practically at the origin, 25 ± 180 Ma). This age of 471 Ma is interpreted as the crystallisation age of this metagranite.

Metaleucogranite BAS 1

The BAS-1 transition gneiss is a two-mica metaleucogranite. Its texture is equigranular to augen, and it forms a "sill", slightly discordant to the stratification of the mica schist and limestone, in the basal member of the Canaveilles Formation, some 150 m above the G2 – G1 Carança gneiss. The abundant but small zircons in this rock are transparent, pink to lilac coloured, and well formed. They represent a population grouped together in the top left of the typological diagram. In all, 56% of the zircons were indexed (fig. 2c). The average population index I.A,I.T (alkalinity and temperature indices) = 241-369 corresponds to the area of the crustal anatexis at the origin of the aluminous leucocratic granites. Five fractions of three to six crystals selected amongst the least magnetic were analysed.

Fractions 2, 3 and 4 are well aligned and indicate identical $^{207}Pb/^{206}Pb$ ages of 467 Ma. Fraction 2 plots along the Concordia. Fractions 1 and 5 have older $^{207}Pb/^{206}Pb$ ages (517 and 560 Ma), indicating an inherited component in this rock, in agreement with its crustal origin. The regression by points 2, 3 and 4 cuts through the Concordia (table II, fig. 3b) with an upper intercept at 467 ± 7 Ma (the lower intercept is located at the origin, 10 ± 280 Ma). This age of 467 Ma is interpreted as corresponding to the crystallisation age of this metaleucogranite.

Metaleucogranite (LP 1)

Sample LP 1 corresponds to a G1-La-Preste-type orthogneiss of coarse-grained muscovite- and biotite-bearing porphyritic leucogranite, showing a slightly schistose facies and a preserved "intrusive" contact with andalusite- and biotite-bearing mica schist, but without signs of contact metamorphism. The zircons in this rock are transparent and euhedral, but commonly rounded, and therefore cannot be classified according to the typological scheme of Pupin [1980]; the majority of those that could be classified are of the S1-2, S6 and S11-12 type. The average population index I.A,I.T = 262-433 corresponds to the field related to crustal anatexis that generated the aluminous granites (fig. 2c).

Seventeen points were analysed (SHRIMP) on 13 different grains (tables III and IV). The cathodoluminescence photos enabled the inherited cores to be identified. Grain 2 is representative of the majority population without an inherited core (fig. 4). In addition to the complexity due to detrital zircons, there is also that of common Pb, as for analysis 2.1, but the induced displacement of the points in the Concordia diagram of Tera and Wasserburg [1972] (fig. 5a) not corrected for common Pb, is easy to interpret. Another difficulty in the interpretation of data is linked to the loss of radiogenic Pb (Pb*): four points (9.1, 10.1, 10.2

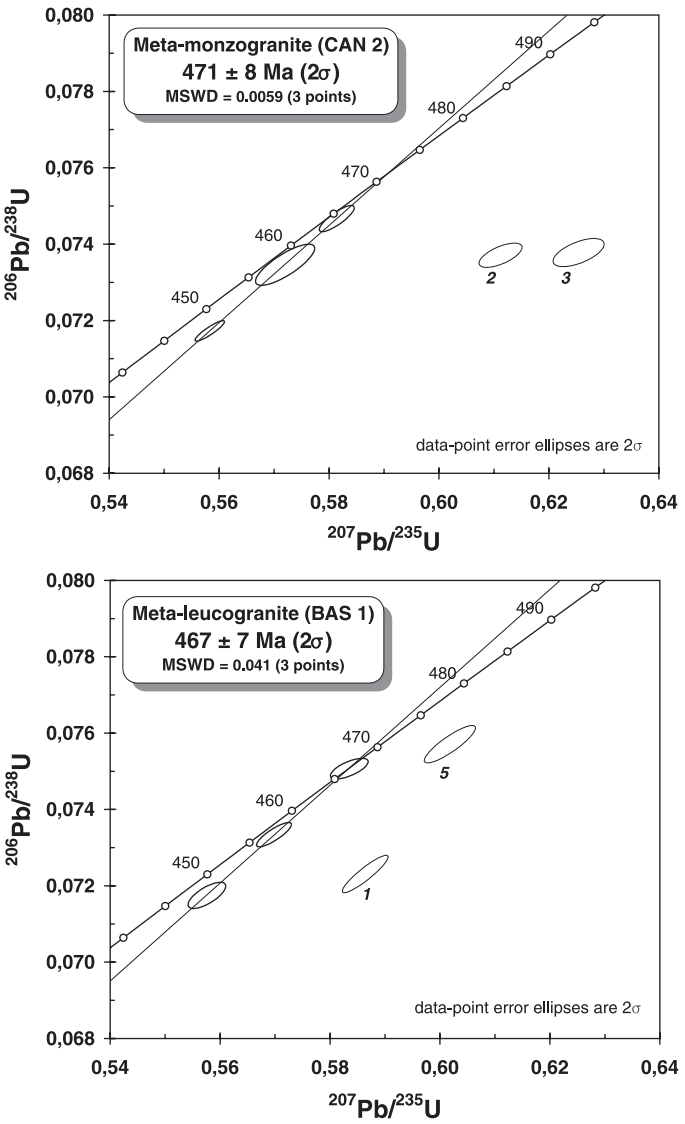

FIG. 3. – Conventional $^{206}Pb^*/^{238}U$ *vs.* $^{207}Pb^*/^{235}U$ Concordia diagram, data from ID-TIMS : a) CAN 2, meta-monzogranite; b) BAS 1, meta-leucogranite.

FIG. 3. – *Diagramme concordia* $^{206}Pb^*/^{238}U$ *vs.* $^{207}Pb^*/^{235}U$*, pour les données par TIMS sur zircons par dilution isotopique et dissolution* a) *CAN 2, méta-monzogranite;* b) *BAS 1, méta-leucogranite.*

and 13.1) are significantly affected by this loss of Pb*. The major event is clearly given by the intersection of the line drawn on the basis of the $^{207}Pb/^{206}Pb$ ratio value of the common Pb, as given by Stacey and Kramers' model (at an age similar to that of the sought event, i.e. here around 470 Ma), and of the five analytical points near the Concordia. The mixing line drawn (fig. 5a) gives a well-defined lower intercept at 477 ± 4 Ma, calculated on eight points. This diagram clearly shows that the progressive trend observed on these eight analyses is due to common Pb and not to the mixing line with the points corresponding to the inherited zircons.

Grains 4 and 5 have inherited cores (fig. 4) dated at around Cambrian-Proterozoic boundary. The detrital zircon domains were respectively dated at 546 ± 14 Ma (4.2) and 631 ± 15 Ma (5.2). These ages are well constrained and significantly different in so far as they are concordant in the

TABLE III. – SHRIMP U-Pb zircon data for sample from Pyrénées and Montagne Noire. Analyses in italic were not considered for average age calculation.
TABL. III. – *Analyses U-Pb (SHRIMP) sur zircon pour les échantillons des Pyrénées et de la Montagne noire. Les analyses en italiques n'ont pas été prises en considération pour le calcul des âges.*

							Total				Radiogenic		Age (Ma)	
Grain. spot	U (ppm)	Th (ppm)	Th/U	Pb* (ppm)	$^{204}Pb/^{206}Pb$	f_{206} % [2]	$^{238}U/^{206}Pb$	± [1]	$^{207}Pb/^{206}Pb$	± [1]	$^{206}Pb/^{238}U$ [3]	± [1]	$^{206}Pb/^{238}U$	± [1]
Meta-leucogranite LP 1														
1,1	564	75	0,13	40	0,00024	0,34	13,13	0,19	0,0589	0,0007	0,0759	0,0011	472	7
2,1	487	271	0,56	39	0,0014	2,63	12,82	0,17	0,0775	0,0007	0,0760	0,0010	472	6
3,1	969	226	0,23	73	0,0024	4,18	12,25	0,16	0,0900	0,0008	0,0782	0,0010	485	6
4,1	622	204	0,33	48	0,00017	0,07	13,04	0,18	0,0568	0,0005	0,0766	0,0010	476	6
4,2	*1759*	*358*	*0,20*	*144*	*0,00040*	*0,26*	*11,28*	*0,15*	*0,0583*	*0,0006*	*0,0884*	*0,0012*	*546*	*7*
5,1	837	63	0,08	60	0,00008	0,13	12,92	0,18	0,0572	0,0004	0,0773	0,0011	480	6
5,2	*1429*	*570*	*0,40*	*148*	*0,00006*	*0,61*	*9,67*	*0,12*	*0,0612*	*0,0004*	*0,1028*	*0,0013*	*631*	*8*
7,1	1192	108	0,09	84	0,00055	1,05	12,90	0,17	0,0647	0,0005	0,0767	0,0010	477	6
9,1	*362*	*147*	*0,41*	*26*	*0,00022*	*0,68*	*14,38*	*0,20*	*0,0617*	*0,0006*	*0,0691*	*0,0010*	*431*	*6*
10,1	*587*	*45*	*0,08*	*39*	*0,00023*	*0,29*	*13,77*	*0,18*	*0,0585*	*0,0005*	*0,0724*	*0,0010*	*451*	*6*
10,2	*442*	*36*	*0,08*	*29*	*0,00020*	*0,49*	*14,25*	*0,19*	*0,0602*	*0,0006*	*0,0698*	*0,0010*	*435*	*6*
11,1	953	63	0,07	69	0,00017	0,17	12,72	0,16	0,0576	0,0004	0,0785	0,0010	487	6
12,1	1171	533	0,46	90	0,00015	0,15	13,36	0,18	0,0574	0,0004	0,0748	0,0010	465	6
13,1	*1046*	*83*	*0,08*	*71*	*0,00010*	*0,10*	*13,70*	*0,18*	*0,0570*	*0,0004*	*0,0729*	*0,0010*	*454*	*6*
Meta-microgranite LP 2														
1,1	*930*	*62*	*0,07*	*79*	*0,00006*	*0,16*	*13,98*	*0,15*	*0,0575*	*0,0005*	*0,0714*	*0,0008*	*445*	*5*
2,1	1393	94	0,07	128	0,00001	<0.01	13,01	0,14	0,0556	0,0003	0,0769	0,0008	478	5
3,1	*810*	*64*	*0,08*	*80*	*0,00001*	*0,71*	*11,96*	*0,14*	*0,0635*	*0,0005*	*0,0830*	*0,0009*	*514*	*6*
4,1	507	38	0,07	45	0,00006	0,03	13,46	0,16	0,0565	0,0005	0,0743	0,0009	462	5
5,1	*564*	*82*	*0,14*	*50*	*0,00003*	*0,11*	*13,67*	*0,16*	*0,0571*	*0,0004*	*0,0731*	*0,0009*	*455*	*5*
5,2	*322*	*108*	*0,33*	*41*	*0,00006*	*<0.01*	*10,14*	*0,14*	*0,0595*	*0,0008*	*0,0987*	*0,0013*	*607*	*8*
6,1	517	55	0,11	46	0,00002	<0.01	13,53	0,16	0,0560	0,0005	0,0740	0,0009	460	5
7,1	719	65	0,09	64	0,00009	0,08	13,50	0,15	0,0568	0,0005	0,0740	0,0008	460	5
8,1	*541*	*41*	*0,08*	*31*	*0,00003*	*0,12*	*14,12*	*0,16*	*0,0572*	*0,0004*	*0,0708*	*0,0008*	*441*	*5*
9,1	*140*	*74*	*0,53*	*11*	*0,000002*	*1,27*	*11,26*	*0,60*	*0,0686*	*0,0021*	*0,0877*	*0,0047*	*542*	*28*
9,2	514	40	0,08	31	0,00003	<0.01	13,27	0,15	0,0561	0,0007	0,0754	0,0009	468	5
10,1	142	100	0,70	10	0,00001	0,14	13,27	0,19	0,0573	0,0007	0,0752	0,0011	468	6
11,1	611	46	0,08	38	<0.000001	<0.01	13,13	0,16	0,0555	0,0006	0,0762	0,0009	474	5
12,1	673	49	0,07	41	0,00007	0,00	13,08	0,15	0,0562	0,0003	0,0765	0,0009	475	5
13,1	619	497	0,80	47	0,000004	0,01	12,88	0,14	0,0563	0,0003	0,0776	0,0009	482	5
14,4	964	52	0,05	59	0,00010	<0.01	12,99	0,14	0,0561	0,0003	0,0770	0,0008	478	5
15,3	560	44	0,08	35	0,00009	0,11	12,97	0,15	0,0571	0,0005	0,0770	0,0009	478	5
Meta-monzogranite SOM 1														
1,1	1311	55	0,04	85	<0.000001	<0.01	13,25	0,17	0,0564	0,0004	0,0755	0,0010	469	6
2,1	*748*	*171*	*0,23*	*112*	*<0.000001*	*<0.01*	*5,73*	*0,07*	*0,0730*	*0,0004*	*0,1746*	*0,0024*	*1037*	*13*
2,2	*220*	*41*	*0,19*	*33*	*0,00007*	*0,30*	*5,80*	*0,13*	*0,0758*	*0,0021*	*0,1719*	*0,0039*	*1022*	*21*
3,1	284	68	0,24	19	<0.000001	<0.01	13,00	0,19	0,0566	0,0008	0,0769	0,0011	478	7
4,1	494	25	0,05	32	<0.000001	<0.01	13,29	0,19	0,0562	0,0009	0,0752	0,0011	468	6
5,1	975	65	0,07	64	0,00084	1,68	13,18	0,17	0,0699	0,0010	0,0746	0,0010	464	6
5,2	1141	48	0,04	74	0,00005	0,04	13,19	0,17	0,0568	0,0004	0,0758	0,0010	471	6
5,3	859	31	0,04	56	<0.000001	<0.01	13,08	0,17	0,0563	0,0005	0,0765	0,0010	475	6
6,1	602	26	0,04	38	0,00019	0,53	13,46	0,18	0,0605	0,0006	0,0739	0,0010	460	6
7,1	331	21	0,06	22	0,00010	<0.01	13,06	0,18	0,0560	0,0007	0,0766	0,0011	476	7
8,1	1283	30	0,02	86	0,00015	<0.01	12,86	0,17	0,0565	0,0005	0,0778	0,0010	483	6
9,1	392	37	0,09	26	<0.000001	0,22	13,19	0,18	0,0583	0,0007	0,0756	0,0011	470	6
Meta-rhyodacite GRA 1														
2,1	*242*	*205*	*0,85*	*36*	*0,00005*	*0,05*	*9,97*	*0,13*	*0,0620*	*0,0007*	*0,1002*	*0,0013*	*616*	*8*
3,1	*156*	*71*	*0,45*	*18*	*0,00006*	*0,21*	*11,25*	*0,18*	*0,0602*	*0,0008*	*0,0887*	*0,0014*	*548*	*8*
3,2	147	65	0,44	12	0,00017	0,30	10,68	0,14	0,0610	0,0011	0,0933	0,0012	575	7
4,1	*361*	*310*	*0,86*	*89*	*0,00002*	*<0.01*	*6,05*	*0,07*	*0,0734*	*0,0005*	*0,1655*	*0,0020*	*987*	*11*
5,1	*174*	*97*	*0,56*	*29*	*0,00011*	*0,12*	*8,21*	*0,11*	*0,0668*	*0,0006*	*0,1216*	*0,0017*	*740*	*10*
7,1	*708*	*49*	*0,07*	*75*	*0,00002*	*<0.01*	*11,30*	*0,13*	*0,0584*	*0,0004*	*0,0885*	*0,0010*	*547*	*6*
7,2	510	280	0,55	63	<0.000001	0,06	10,95	0,14	0,0590	0,0004	0,0913	0,0011	563	7
8,1	208	89	0,43	18	0,00001	<0.01	10,36	0,15	0,0571	0,0009	0,0967	0,0014	595	8
8,2	248	113	0,46	21	0,00011	0,27	10,68	0,14	0,0607	0,0006	0,0934	0,0012	576	7
9,1	174	72	0,41	15	0,00013	0,18	10,38	0,16	0,0600	0,0007	0,0962	0,0015	592	9
9,2	147	51	0,35	12	0,00021	0,16	10,55	0,14	0,0599	0,0009	0,0946	0,0013	583	8
10,1	144	38	0,26	12	0,00028	0,35	10,41	0,16	0,0614	0,0007	0,0957	0,0015	589	9
10,2	*211*	*145*	*0,69*	*20*	*0,00018*	*0,31*	*9,96*	*0,12*	*0,0611*	*0,0006*	*0,1000*	*0,0013*	*615*	*7*
11,1	*262*	*98*	*0,37*	*40*	*0,00003*	*<0.01*	*5,80*	*0,07*	*0,0735*	*0,0005*	*0,1726*	*0,0021*	*1026*	*12*
13,1	149	63	0,42	12	0,00004	0,26	10,84	0,16	0,0606	0,0012	0,0920	0,0014	568	8

[1] Uncertainties given at one σ level
[2] f_{206} % denotes the percentage of ^{206}Pb that is common Pb
[3] Correction for common Pb made using the measured $^{238}U/^{206}Pb$ et $^{207}Pb/^{206}Pb$ ratios following Tera & Wasserburg [1972] as outlined in Williams [1998]

diagram of Tera and Wasserburg [1972]. It should be noted that on each of these two grains we analysed a second point, closer to the pyramid of the grain, which this time gave the same Ordovician age of 476 ± 12 Ma (4.1) and 480 ± 12 Ma (5.1) respectively (fig. 5a). As explained in the analytical section, the inherited domains (older than 1000 Ma) are more likely plotted using the conventional Concordia diagram (fig. 6a). Then, we can observe that the analyses obtained on grains 6 and 8 line up within the limit of errors on a Discordia that does not go through the origin (fig. 6a). The upper intercept defines an age of 2032 ± 11 Ma, whereas the lower intercept defines an age of around 400 Ma (367 + 86-89 Ma). Within the limit of error on this young age, it could be considered to correspond to the age of

TABLE IV. – SHRIMP U-Pb zircon data for inherited grains from Pyrénées for ages older than "Cadomian".
TABL. IV. – *Analyses U-Pb (SHRIMP) sur zircons hérités des Pyrénées antérieurs pour des âges antérieurs au Cadomien.*

Grain. spot	U (ppm)	Th (ppm)	Th/U	Pb* (ppm)	$^{204}Pb/^{206}Pb$	f_{206} % [2]	Radiogenic ratios $^{206}Pb/^{238}U$ [3]	± [1]	$^{207}Pb/^{235}U$ [3]	± [1]	$^{207}Pb/^{206}Pb$ [3]	± [1]	Ages (Ma) $^{206}Pb/^{238}U$	± [1]	$^{207}Pb/^{235}U$	± [1]	$^{207}Pb/^{206}Pb$	± [1]	Conc. % [4]
Meta-leucogranite LP 1																			
6,1	304	388	1,27	140	0,00016	0,30	0,3585	0,0053	6,151	0,101	0,1245	0,0007	1975	25	1997	14	2021	9	98
6,2	468	656	1,40	205	0,00013	0,24	0,3334	0,0051	5,710	0,096	0,1242	0,0007	1855	25	1933	15	2018	10	92
8,1	627	446	0,71	211	0,000040	0,07	0,2963	0,0040	4,974	0,072	0,1218	0,0005	1673	20	1815	12	1982	7	84
Meta-microgranite LP 2																			
3,2	779	244	0,31	452	0,000019	0,03	0,4197	0,0047	9,139	0,122	0,1579	0,0010	2259	21	2352	12	2433	10	93
14,1	332	198	0,60	212	0,000001	<0.01	0,5904	0,0137	23,404	0,749	0,2875	0,0056	2991	56	3244	32	3404	31	88
14,2	190	56	0,29	84	0,000015	0,02	0,4307	0,0081	15,403	0,390	0,2594	0,0038	2309	37	2841	24	3243	23	71
14,3	1670	32	0,02	321	0,000006	<0.01	0,2250	0,0028	4,377	0,060	0,1411	0,0006	1308	15	1708	11	2240	8	58
14,5	804	78	0,10	281	0,000001	<0.01	0,3947	0,0046	8,816	0,121	0,1620	0,0010	2145	21	2319	13	2477	10	87
15,1	300	89	0,30	99	0,000009	0,01	0,3638	0,0046	6,192	0,099	0,1234	0,0010	2000	22	2003	14	2007	15	100
15,2	1198	372	0,31	323	0,000018	0,02	0,2985	0,0033	4,924	0,067	0,1196	0,0008	1684	16	1806	12	1951	12	86
Meta-rhyodacite GRA 1																			
1,1	608	470	0,77	116	0,000017	0,03	0,1321	0,0016	1,188	0,016	0,0652	0,0003	800	9	795	7	782	11	102
4,1	361	310	0,86	88	0,000022	0,04	0,1652	0,0020	1,664	0,024	0,0731	0,0005	986	11	995	9	1015	15	97
5,1	174	97	0,56	29	0,00011	0,19	0,1216	0,0017	1,093	0,022	0,0652	0,0009	740	10	750	11	781	29	95
6,1	109	238	2,19	102	0,000093	0,13	0,4764	0,0077	10,645	0,242	0,1621	0,0023	2512	34	2493	21	2477	24	101
6,2	413	150	0,36	332	0,000004	0,01	0,5557	0,0068	15,207	0,208	0,1985	0,0010	2849	28	2828	13	2814	8	101
11,1	262	98	0,37	40	0,000026	0,05	0,1723	0,0021	1,738	0,026	0,0731	0,0006	1025	12	1023	10	1017	15	101
12,1	238	76	0,32	91	0,000010	0,01	0,4107	0,0059	9,136	0,153	0,1613	0,0012	2218	27	2352	15	2470	12	90

[1] Uncertainties given at one σ level
[2] f_{206} % denotes the percentage of ^{206}Pb that is common Pb
[3] Correction for common Pb made using the measured $^{204}Pb/^{206}Pb$ ratio
[4] For % Conc., 100% denotes a concordant analysis.

477 Ma calculated in the Tera and Wasserburg [1972] diagram. This *in situ* approach therefore made it possible to date, with precision, the early Ordovician crystallisation age of the majority of the magmatic zircons in this metaleucogranite at 477 ± 4 Ma. A Proterozoic heritage is highlighted at 2032 ± 11 Ma. Other, more recent inherited components are also clearly identified at around 550 and 630 Ma.

Metamicrogranite LP 2

Sample LP 2 is an orthogneiss of the G1-La-Preste-type aluminous porphyritic microgranite, running as veins through the G1 gneiss of Carança. The zircons in this rock are abundant; some are transparent and asymmetrical while many others are corroded and stippled on their surface. They mainly show a characteristic S1-S2-S6 shape type according to the morphological typology of Pupin [1980]. Like the LP 1 facies, these zircons plot in the field of crustal anatectic granites (fig. 2c).

Twenty four points were analysed on 15 different grains. The combination of cathodoluminescence photos and the analyses shown in the Tera and Wasserburg [1972] Concordia diagram (fig. 5b) led us to identify several inherited core zircons (grains 3, 5, 14 and 15). On the other hand, the majority of the grains gave, within the age error limit, identical $^{206}Pb^*/^{238}U$ ages (table III). Three points (1.1, 5.1, and 8.1) were affected by a slight loss of Pb* and are not taken into consideration for mean age calculation (fig. 5b). The major event was dated by means of 11 concordant analyses: the precise measurement of the $^{207}Pb/^{206}Pb$ ratio showed the absence of common Pb in these analyses. The average $^{206}Pb^*/^{238}U$ age, given by the intercept of the mixing line with the common Pb and the population of 11 analyses, was therefore well defined at 472 ± 6 Ma. This age is interpreted as corresponding to the crystallisation age of this metagranite.

Figure 5b shows two analyses (3.1 and 9.1) that plot along a mixing line with the points of the inherited zircons. A concordant point (5.2) can also be seen, for which the age of 607 ± 16 Ma is significant. The other analyses on inherited zircons gave much older ages: they would be more suitably dealt with in a conventional Concordia diagram (fig. 6b). The zircon 14 was interesting for two reasons firstly, it provided very important data concerning the ages of various inherited components and, secondly, it enabled a better understanding of the successive processes of reopening of the U-Pb system in a zircon. An inherited core is also revealed by the cathodoluminescence photo (fig. 4). Correlatively, the five analyses carried out on this grain showed an inherited core (14.1) with a minimum age of 3404 Ma (fig. 6b) and a late crystallisation episode, from the exactly concordant analysis (14.4) of 478 ± 10 Ma, to be compared with the average $^{206}Pb/^{238}U$ age obtained on eleven analyses of 472 ± 6 Ma. The three other analyses were discordant and, consequently, more difficult to interpret. Similar discordant analyses (fractions 2 and 3), obtained by ID-TIMS for metamonzogranite sample CAN 2 could not be interpreted (see section CAN 2). However, the combination of a careful examination of the distribution of the five SHRIMP analyses of grain 14 in the Concordia diagram (fig. 6b) and the cathodoluminescence study of the corresponding domains allows a more refined interpretation, without invoking continuous losses through diffusion of radiogenic Pb. One observes that the light central part of the grain enabled two measurements to be carried out that line up with a third carried out in the darkest part of the grain (14.3), very rich in U (1670 ppm) and apparently the most discordant. Finally, in an intermediate area between this internal dark part and the external zone dated at 478 Ma, an

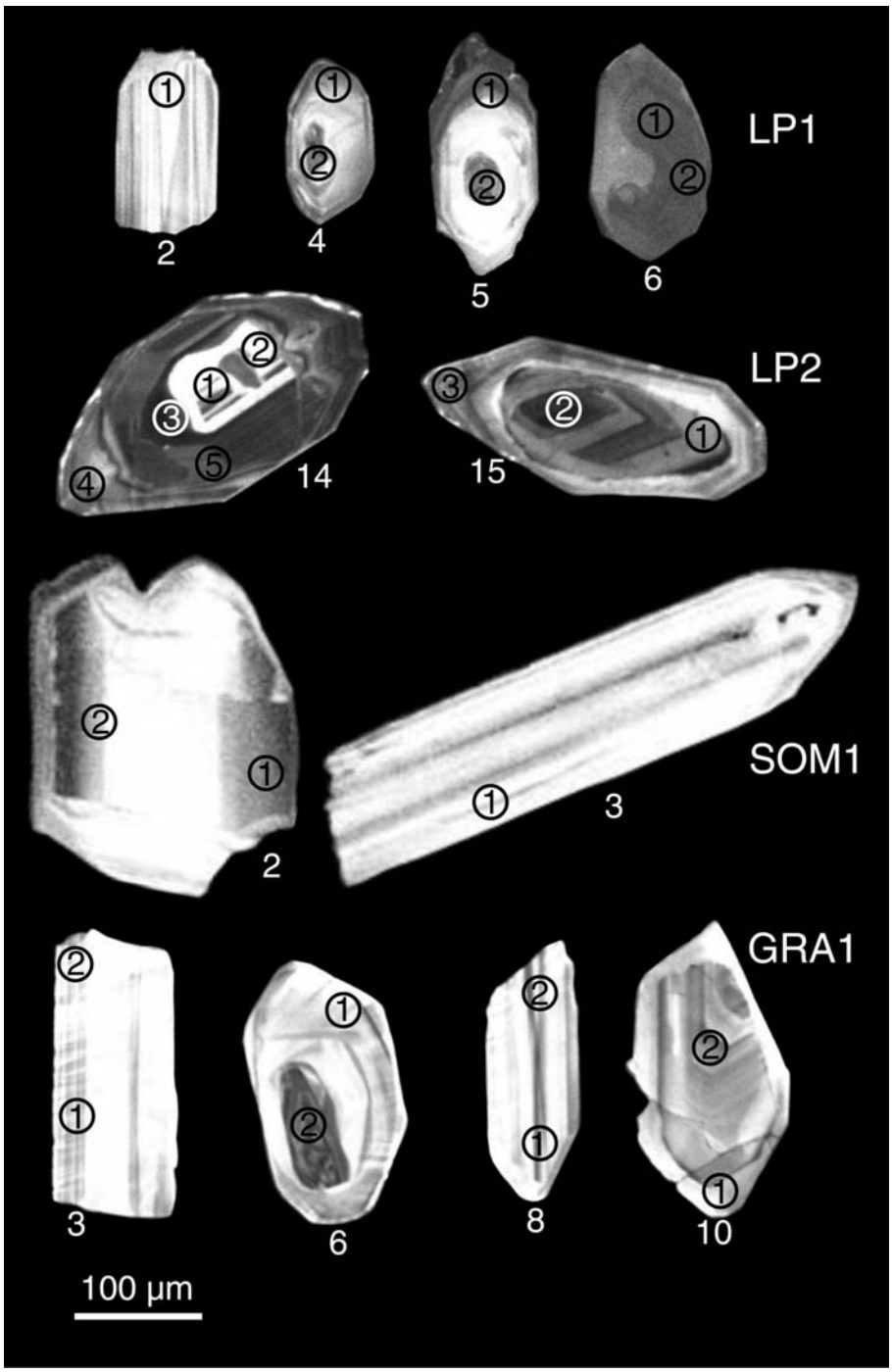

FIG. 4. – Representative cathodoluminescence images of zircon grains analysed using SHRIMP II. Spot size is 20-25 µm. LP 1: grains 2, 4, 5 and 6; LP 2: grains 14 and 15; SOM 1: grains 2 and 3; GRA 1: grains 3, 6, 8 and 10.
FIG. 4. – *Images en cathodoluminescence représentatives de quelques zircons analysés à l'aide de la SHRIMP II. La dimension du domaine analysé est de 20-25 µm.* LP 1 : *grains 2, 4, 5 et 6 ;* LP 2 : *grains 14 et 15 ;* SOM 1 : *grains 2 et 3* ; GRA 1 *: grains 3, 6, 8 et 10.*

analysis (14.5; 13 % discordance) gave a minimum age of 2477 Ma (table IV). It is possible to interpret these data as analyses representative of mixtures between homogeneous areas of different ages in relation to the reopening of the system during distinct, successively recorded thermal events. One observes that the very dark area does not only edge the light and very old part of the grain: part of this area extends up to the periphery of the grain (fig. 4, bottom right). Consequently, this dark area is in reality more recent than the area represented by analysis 14.5. One may therefore trace a Discordia or, more exactly, a mixing line, between analyses 14.1, 14.2 and 14.3. The two poles of the mixing line give, by the upper intercept, the oldest inherited age of 3512 ± 54 Ma and, by the lower intercept, an important thermal event that led to the reopening of the system at 1046 ± 34 Ma. This latter type of heritage, for example, was revealed by two concordant analyses at 1033 ± 22 Ma on a zircon from the SOM 1 orthogneiss and on a zircon, also concordant at 1016 ± 30 Ma, from the metavolcanite GRA 1 (following §). Then, if the mixing line between the two analyses 14.5 and 14.4 is traced, then a third inherited age of 2511 ± 17 Ma is obtained by the upper intercept. Apart from analysis 14.4 carried out on a completely homogeneous and concordant area, it can be seen that the four other discordant analyses may be interpreted in terms of mixtures. Thus, despite the good spatial resolution of the

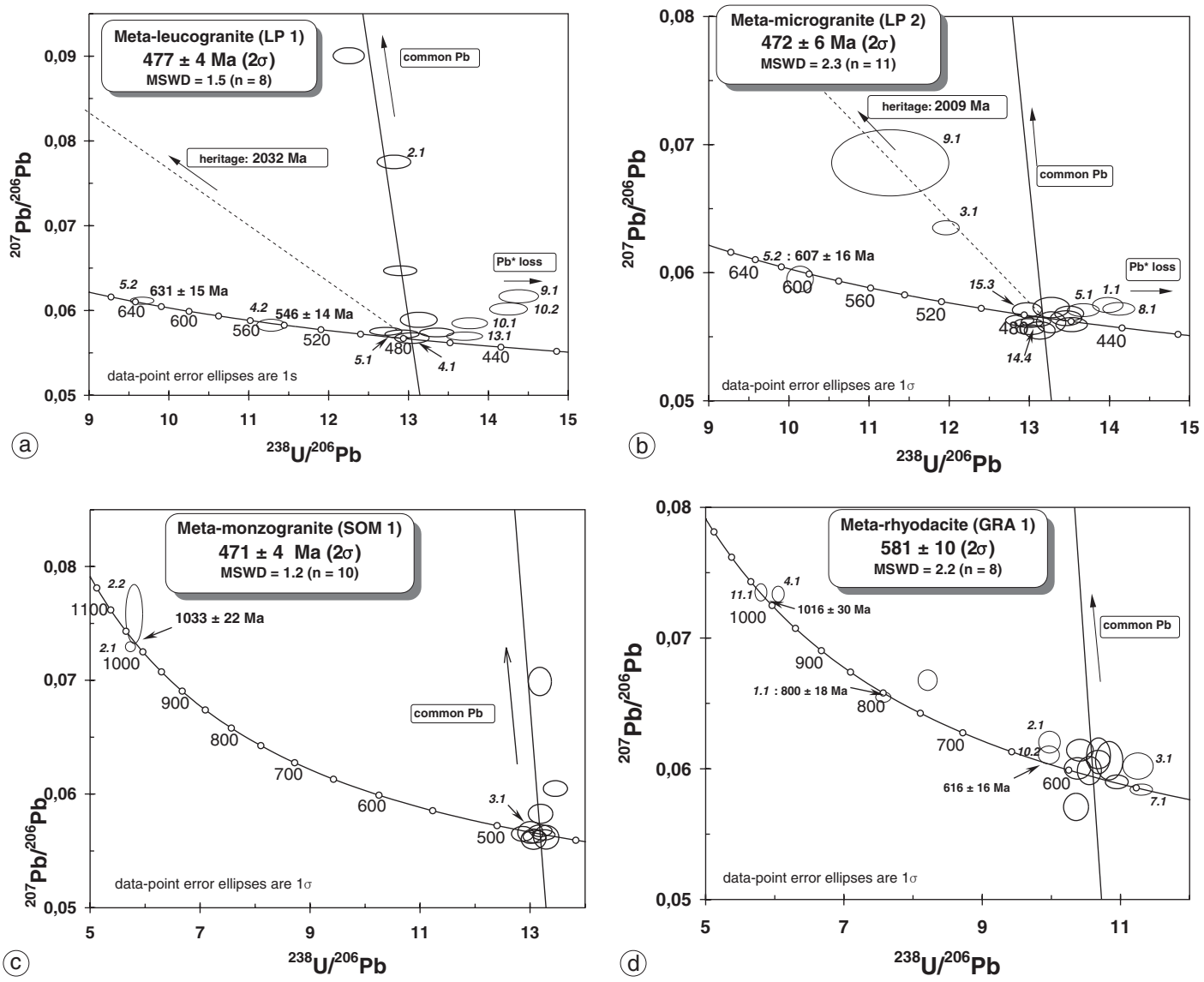

FIG. 5. – Common Pb uncorrected Tera and Wasserburg [1972] diagram for data obtained with SHRIMP II on zircon grains from various orthogneiss: a) metaleucogranite LP 1; b) metamicrogranite LP 2; c) metamonzogranite SOM 1; d) metatuff-rhyodacite GRA 1. Data error ellipses drawn at 1σ, but calculation done at the 2σ level. "Light" ellipses are not taken into account for the average age calculation. Heavy lines correspond to evolution trends from zircon analyses without common Pb up to full common Pb composition [Stacey and Kramers, 1975]. Dashed lines represent theoretical mixing lines from calculated Ordovician ages (TW) towards inherited ages calculated using conventional Concordia diagram for zircon domains older than 1000 Ma.
FIG. 5. – *Diagramme de Tera et Wasserburg non corrigé du Pb commun. Les données ont été obtenues à l'aide de la SHRIMP II sur zircons de divers orthogneiss :* a) *méta-leucogranite LP 1 ;* b) *métamicrogranite LP 2 ;* c) *métaleucogranite SOM 1 ;* d) *métatuf-rhyodacite GRA 1. Les ellipses d'erreur sont données à 1σ, mais les calculs d'erreur sur les âges sont faits à 2σ. Les ellipses en traits légers n'ont pas été prises en compte pour le calcul de l'age moyen. En traits pleins sont représentées les droites d'évolution depuis les analyses concordantes dépourvues de Pb commun jusqu'à la composition du Pb commun à l'âge supposé des zircons [Stacey et Kramers, 1975]. En tiretés sont représentées les droites de mélange théoriques entre les âges ordoviciens calculés (TW) et les âges hérités calculés à partir des diagrammes Concordia conventionnels pour les domaines plus anciens que 1000 Ma.*

SHRIMP, it was not always possible to work on completely homogeneous zones, although with the help of the cathodoluminescence image, it is sometimes possible to interpret such discordant analyses.

The power of the SHRIMP method was demonstrated by the study of grain 15, which has an inherited core, but a simpler history. Two of the three analyses carried out were concordant at 478 ± 10 Ma and 2007 ± 30 Ma (table III). The third analysis is located exactly on the mixing line between these two poles. This Discordia confirms the Ordovician age (472 ± 6 Ma) and makes it possible to calculate a new inherited age of 2009 ± 24 Ma (fig. 6b). A fracture from the core of the grain, which does not extend to the more recent border of the grain, is observed by cathodoluminescence (fig. 4) at the spot where analysis 15.2 was carried out. This suggests that the isotopic system was partially rejuvenated in the Ordovician in this precise zone, whereas the area corresponding to analysis 15.1 remained completely closed.

Metamonzogranite SOM 1

Sample SOM 1 is an augen orthogneiss derived from a two-mica porphyritic monzogranite of the southern part of

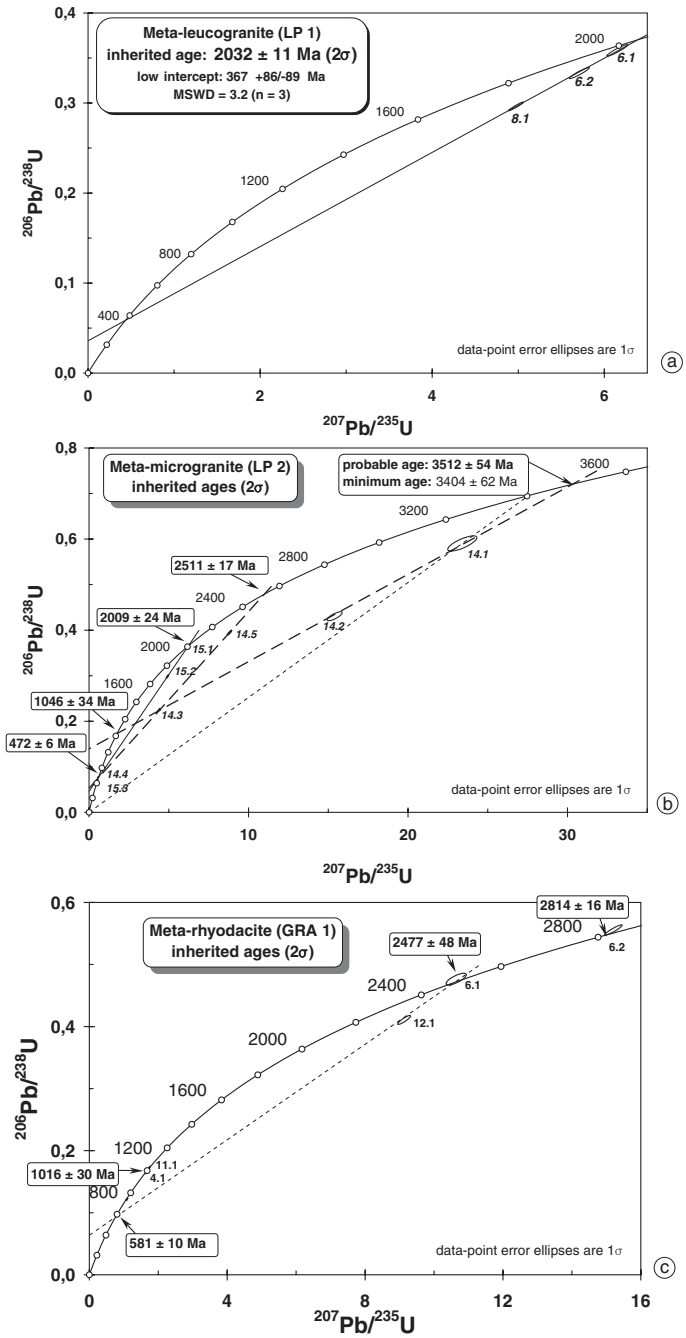

FIG. 6. – Conventional $^{206}Pb^*/^{238}U$ *vs.* $^{207}Pb^*/^{235}U$ Concordia diagram, data from zircons of inherited origin obtained with SHRIMP II on zircon grains from: a) metaleucogranite LP 1; b) metamicrogranite LP 2; c) metatuff rhyodacite GRA 1. Error ellipses are given at 1σ, but the calculations are made at 2σ.

FIG. 6. – *Diagramme Concordia conventionnel* $^{206}Pb^*/^{238}U$ *vs.* $^{207}Pb^*/^{235}U$ *pour les analyses issues de zircons hérités obtenues à l'aide de la SHRIMP II* : a) *métaleucogranite* LP 1 ; b) *métamicrogranite* LP 2 ; c) *métatuf-rhyodacite GRA 1. Les ellipses d'erreur sont données à 1σ, mais les calculs sont faits à 2σ.*

the Montagne Noire Axial Zone. The cm-sized K-feldspar megacrysts do not show any evidence of anatectic overprinting. The zircons in this rock are elongated and well formed, while others are thickest and locally deformed, commonly quite large 200-300 µm, transparent and colourless. The elongate zircons are often broken (fig. 4). The morphological typology according to Pupin's classification [1980] indicates a maximum of S2-S6 type specimens. Nearly 50% of the grains could be indexed: the average population index I.A,I.T = 295-379 corresponds to the field of crustal anatectic granitoids. Twelve points were analysed on nine different grains. Twelve analyses (table III) showed the virtual absence of common Pb, except in the case of one analysis (5.1). In the Tera and Wasserburg [1972] diagram (fig. 5c), two analysis groups are distinguished. The first one only comprises two analyses (2.1 and 2.2) stemming from the same grain. These analyses were in agreement and give a unique age, meaning that it is probably significant of a geological age, although it is quite imprecise at 1033 ± 22 Ma due to the limited data. The second group, of which grain 3 is representative (fig. 4), corresponds to all the other analyses. Certainly, two of the 10 remaining analyses are significantly affected by the presence of common Pb, but they still may be used thanks to this graphic representation, since they are located on the progressive trend from the group of concordant points to the composition in common Pb during the Ordovician. No trace of Pb loss appears and no trace of detrital zircon is visible in this homogeneous population. The age calculated at the intercept between the Concordia and the mixing line with common Pb gives a tightly grouped age over 10 analyses of 471 ± 4 Ma. This age is interpreted as corresponding to the crystallisation age of this orthogneiss.

Rhyodacitic metatuff GRA 1

Sample GRA 1 is a metatuff containing homogeneous lapilli (~85%) in a very fine matrix (≤15%). It is massive, shows very little deformation, and is affected by the biotite metamorphism of the pluton of St. Laurent de Cerdans. The lapilli, of 4 to 6 mm, are practically non deformed and unworn by transport, very homogeneous, with small albitised K-feldspar and albite phenocrysts in a fine quartz-albite and biotite mesostasis. The lapilli matrix is slightly schistose, containing biotite, leucoxene, clinozoisite and graphite apparently of a clay type, like the surrounding black sediments that embedded this tuffite of more than 150 m thick.

The zircons in this rock are quite numerous, commonly small and highly coloured and locally transparent or corroded on the surface. According to the morphological typology of Pupin [1980], the most represented types are located in S1-S2 and S6-S11-S12. Only 35 % of the grains could be indexed: the average population index I.A,I.T = 285-454 corresponds to the domain of crustal anatetic granites (fig. 2a). Nineteen spots were analysed on 13 different grains (tables III and IV). The cathodoluminescence photos taken enabled inherited cores (e.g. grain 6, fig. 4) to be identified. The analyses were practically all concordant (fig. 5d). The majority of the points analysed (12) are grouped together on the Concordia around 600 Ma. On the other hand, the dispersion of these points is much greater than the analytical uncertainties. The analysis of grains 3 and 8, for example, reflects this age dispersion: 548, 575, 595, 576 Ma, whereas the internal structures of these grains appear very simple (fig. 4). On the other hand, analysis 10.2 and the corresponding photo lead one to consider the existence of an inherited internal structure. In the same way, analysis 2.1 was not retained for calculating the average age (fig. 5d). The 10 remaining concordant analyses gave a

$^{206}Pb^*/^{238}U$ age of 574 ± 13 Ma, but the MSWD is high (5.3), showing that this age poses a problem of interpretation. From a statistical point of view, an MSWD greater than 2 for a population of 10 analyses does not allow the average calculated age to be interpreted as a unique event [Wendt and Carl, 1991]. In this case, either a slight loss of radiogenic Pb was suffered by the samples leading to the more recent ages, or the volcanic activity continued for 20-30 Ma. We do not consider this latter hypothesis very realistic: indeed, it is highly unlikely that different generations of lavas could be preserved in this sample of tuff with such homogeneous lapilli in a very fine argillo-carbonate matrix. Similarly, it is difficult to envisage that the formation could date from 550-560 Ma and that all of the many more zircons dated between 570 and 600 Ma could be inherited zircons. Consequently, we prefer to consider that the two analyses (3.1 and 7.1) correspond to areas that have suffered a loss of radiogenic Pb. Thus, if one considers the eight remaining analyses, a realistic mean age of 581 ± 10 Ma can be calculated, with an MSWD of 2.2. Therefore, one may assume that this metarhyodacite was formed around 580 Ma. The inherited zircons are once again numerous (fig. 5d) and significant since generally concordant. The most recent are dated at 800 ± 18 Ma and 1016 ± 30 Ma (fig. 5d). The zircon 6 enabled the measurement of two concordant points, but with very significantly different ages (fig. 6c): one around 2800 Ma and the other around 2500 Ma. A third analysis (12.1) lines up with analysis 6.1 and the group of points at 550-600 Ma.

DISCUSSION AND CONCLUSIONS

The five datings of the present study carried out on orthogneisses (Canigou, Roc de France and Montagne Noire) using conventional U-Pb method after dissolution and isotope dilution of zircons and the *in situ* U-Pb zircon method by ion microprobe (SHRIMP) are clearly grouped together around 471 Ma. According to the new international stratigraphic chart [Gradstein and Ogg, 2004], this age marks the early – middle Ordovician boundary (Arenigian – Llanvirnian). A mean weighted age of 473 ± 4 Ma can be assigned to the Pyrenean orthogneisses if we consider our four new age determinations (orthogneiss from Montagne Noire not included) and the 475 ± 10 Ma age determined by Deloule *et al*. [2002]. Concerning the G1-La-Preste (LP1, LP2) and G2 (CAN2) facies and the aluminous leucogranite sills (transition gneiss BAS1), these ages show that the various orthogneisses belong to a single magmatic episode. Thus, the zoning and the progressive character of the changes in the G1, G2 and G3 facies and the sharp contacts of the dykes observed in the field are confirmed as initial emplacement features by virtually identical ages. The three previous datings carried out on the Canigou orthogneiss gave Ordovician ages but substantially more recent ages in two cases obtained by the Pb/Pb zircon evaporation method: 451 ± 14 Ma (CAN1 in fig.1) from 421 ratios [Cocherie *et al*., 1992, *in* Guitard *et al.,* 1996] and 446 ± 20 Ma (LP3 in fig. 1) from 505 ratios [Delaperrière and Respaut, 1995]. However, the 475 ± 10 Ma age obtained by the U-Pb zircon ion microprobe (IMS 1270) from seven analyses on four grains, themselves extracted from three different samples (PY01, PY10 and PY16, fig.1, table I) [Deloule *et al*., 2002], is in complete agreement with our datings.

It should be noted that the most recent ages were obtained using the evaporation method. Within the framework of this method, the isotopic age measurements were obtained without controlling the concordance with the $^{206}Pb/^{238}U$ ratio. Theoretically, the $^{207}Pb^*/^{206}Pb^*$ ages calculated in this way are minimum ages. Nevertheless, particularly in the examples concerned, the evaporation by successive stages made it possible to attain the sought age [Cocherie *et al.,* 1992] with good confidence in so far as several successive stages of heating (3 or 4) gave the same age. Finally, it should be kept in mind that, within the error limit (2σ), the ages of 451 ± 14 Ma (CAN1) and 471 ± 8 Ma (CAN2) cannot really be distinguished at this stage, but leaving a rather wide range of possible ages (~20 Ma). Considering the new four ages obtained by our work, as well as that from Deloule *et al.* [2002], a weighted average age is now much more precisely defined at 473 ± 4 Ma. The two datings of the orthogneiss of the axial zone of the Montagne Noire [Roger *et al.,* 2004 – ID-TIMS method], at the Pont du Larn of 456 ± 3 Ma and in the Gorges d'Héric of 450 ± 6 Ma, also show a younger age dating from the late Ordovician. Our sample (SOM 1), taken from the same facies as that of the Gorges d'Héric, shows a precise *in situ* age of 471 ± 4 Ma, defined with ten analyses including eight concordant analyses, strictly identical to that obtained on the Canigou – Roc de France orthogneiss.

The 581 ± 10 Ma age of the interstratified volcanite layer towards the base of the azoic Canaveilles Group (GRA1) demonstrates, for the first time, the anteriority of these metasediments with regards to the orthogneisses, which may be large laccolithic intrusions. It also confirms the existence of sedimentation dating from the end of the Proterozoic in the Pyrenean Axial Zone, in accordance with the hypothesis of Laumonier [1998], which places the Precambrian-Cambrian boundary towards the upper limit of the Canaveilles Group. The Ordovician microfossils described by Konzalova *et al.* [1982] therefore need to be reinterpreted.

In the Montagne Noire, a metadacite (Sériès tuffs) interbedded within the upper member of the azoic St Pons Cabardès Group, considered by Demange [2003] as an equivalent of the Canaveilles Group, gave an age of 545 ± 15 Ma from 399 ratios (Pb/Pb zircon evaporation method [Lescuyer and Cocherie, 1992]). This result is perfectly compatible with the *in situ* datings of the youngest detrital zircons of this Group at 556 Ma [Gebauer *et al.,* 1989]. The assignment of the St Pons Cabardès Group to the latest Neoproterozoic therefore appears to be established and confirms the stratigraphic equivalence with the Canaveilles Group [Demange, 1988, 2003]. Laumonier *et al.* [2004] provide a more detailed discussion of the consequences of these datings on the validation or the adjustment of the lithostratigraphic succession in these azoic series of southern France.

This study also made it possible to demonstrate the very wide diversity of the sources inherited from the Archaean with the metarhyodacite (GRA 1) and the metamicrogranite (LP 2) up to the "pan-African" or "Cadomian" in the case of zircons from three rocks: the metaleucogranite (LP 1), the metarhyodacite (GRA 1) and the metamicrogranite (LP 2) with ages of 631 ± 5, 607 ± 16, 616 ± 6 and 800 ± 18 Ma.

The "Pyrenees – Montagne Noire" crust portion belongs to the "Iberian – Catalan – Aquitaine" block, known as "Ebroïa", before its Hercynian incorporation to the Iberian-Armorican arc. At the end of the NeoProterozoic (between 600 and 542 Ma [Gradstein and Ogg, 2004]) the northern Gondwanian border (composed, among others, by the future Avalon, Armorica, Ebroïa, etc. terranes) is characterised by an active margin that is identified by a continental arc magmatism and volcano-detrital deposits of the back-arc basin [e.g. Von Raumer *et al.,* 2003; Neubauer, 2002]. To the north of the Armorican Massif, the brief Cadomian tectonic phase (580-540 Ma) could represent the closing of one of these basins. However, during this same period, the Ouarzazate series in the Moroccan Anti-Atlas shows all of the steps of a rifting of the continental back-arc basin, above the subduction of a "proto-Tethys" underneath Gondwana, a basin that evolved under open sea conditions during the Cambrian (upper Adoudou series). It is in this latter, anorogenic context that the Ebroïa block could be situated with the Canaveilles Group located on the distal platform of one of the margins of this basin. The interbedded volcanic deposits inside all the Canaveilles Group, clearly bear witness, as in the Ouarzazate series, to a geochemical back-arc basin affinity [Navidad and Carreras, 2002].

In the Cambrian, the back-arc basin evolved, in its western part, into a true ocean (Rheic) [Von Raumer *et al.,* 2003], leading to the drifting of the Avalon plate. However, towards the east, during the Cambrian and the Ordovician, the whole south European block (including Ebroïa) still remained welded to Gondwana with possible persistence of the active margin to the north [Stampfli and Borel, 2002] and the above mentioned back-arc basin.

Between the early and middle Ordovician, the intense magmatic activity [e.g. Pin and Marini, 1993; Von Raumer *et al.,* 2003; Neubauer, 2002] and the sedimentological variations that characterise all of the south European formations (Massif Armoricain, Massif Central, Alps, Iberia, Pyrenees and the Montagne Noire) argue in favour of their "individualisation" (Hun terranes, [Stampfli, 1996; Stampfli and Borel, 2002]) in relation to the Gondwana margin. Indeed, this margin became particularly apparent during the Ordovician with the persistence of a remarkably homogeneous terrigenous continental platform, stretching from Arabia up to the Moroccan Anti-Atlas. The splitting up and the separation of the south European blocks from the passive north Gondwana margin therefore may be envisaged, from the Ordovician onwards [in agreement with Pin and Marini, 1993]. Of varied chemical composition (hyperalkaline, alkaline, calc-alkaline), the Ordovician magmatism probably bears witness to different geodynamic sites evolving along the Gondwana margin.

The aluminous to calc-alkaline composition of the orthogneiss of the Pyrenees and the Montagne Noire, by virtue of the rarity of basic and tonalitic facies, does not provide any decisive indication as to the geodynamic context of their formation. However, the typology of their "crustal anatexis – S" and/or "calc-alkaline – I" type zircons (fig. 2) and the "Rapakivi" type facies, quite well distributed and symptomatic of crystallisation by mixing of magmas in disequilibrium, suggest their formation by crustal (S) and subcrustal (I) fusion stages in an abnormally high thermal environment. This magmatism evolved at the end of the Ordovician (Dôme de Pierrefitte in the central Pyrenees [Cabanis and Pouit, 1996]) or during the Silurian (in Catalan massif [Gil Ibarguchi *et al.,* 1990]) towards alkaline basalts or alkaline-trend granites, of which the Casemi gneiss in the Massif du Canigou (dated at 425 ± 18 Ma from 1204 ratios [Delaperrière and Soliva, 1992] – Pb zircon evaporation method) are an example.

In the Pyrenees and the Montagne Noire, the unconformity of the late Ordovician on the Cambrian indicates the existence of moderate deformation and a period of emergence that may be linked to an emerged extensional cordillera. It is in such a context of thermal intumescence that the origin of the Ordovician plutonism of the Pyrenees and the Montagne Noire can be understood. A recent example of this kind of magmatism can be observed in the Tertiary granites and volcanoes that crosscut the thick continental crust of the "Colorado Plateau", east of the "Basin and Range" rifted area, and very far from the westerly subduction trench.

Acknowledgements. – We would like to thank M. Demange who shared with us his views on the geology of this part the pre-Hercynian basement. The authors wish to thank P. Jezequel who extracted the zircon grains. We are also indebted to the two anonymous reviewers whose remarks greatly improved the manuscript. We are grateful to R. Stead for polishing the English. This is BRGM contribution No. 3437; the work was financially supported by a BRGM research grant.

References

AUTRAN A., FONTEILLES M. & GUITARD G. (1966). – Discordance du Paléozoïque inférieur métamorphique sur un socle gneissique antéhercynien dans le massif des Albères. – *C. R. Acad. Sci*., Paris, **263**, 317-320.

BARBEY P., CHEILLETZ A. & LAUMONIER B (2001). – The Canigou orthogneisses (eastern Pyrénées, France, Spain): an early Ordovician rakapivi granite laccolith and its contact aureole. – *C. R. Acad. Sci*., Paris, **332**, 129-136.

CABANIS B. & POUIT G. (1996). – Etude géochimique du volcanisme basique ordovicien de Pierrefitte. Le volcanisme anté Stéphanien. *In*: BARNOLAS et CHIRON, Eds., Synthèse géologique et géophysique des Pyrénées. Tome 1. Cycle hercynien. – BRGM-ITGE, Orléans-Madrid, 369-376.

CAVET P. (1957). – Le Paléozoïque de la zone axiale des Pyrénées orientales françaises entre le Roussillon et l'Andorre. – *Bull. Serv. Carte Géol. Fr.*, **254**, 303-518.

CLAUSEN S. & ALVARO J. (2004). – Implications biostratigraphiques et paléobiogéographiques de la découverte du métazoaire néo-Proterozoïque Cloudinia dans le versant nord de la Montagne Noire (France). *In*: *Paléogéographie* – Colloque de l'Académie des sciences et de la Société Géologique de France, Paris, 8-9 Mars 2004, Livre des résumés, 2p.

COCHERIE A., GUERROT C. & ROSSI PH. (1992). – Single-zircon dating by step-wise Pb-evaporation: Comparison with other geochronological techniques applied to the Hercynian granites of Corsica, France. – *Chem. Geol*., **101**, 131-141.

COMPSTON W., WILLIAMS I.S., KIRSCHVINK J.L., ZHANG Z & MA G. (1992). – Zircon U-Pb ages for early Cambrian time scale. – *J. Geol. Soc*., London, **149**, 171-184.

DELAPERRIERE E. & RESPAUT J.-P. (1995). – Un âge ordovicien de l'orthogneiss de La Preste par la méthode d'évaporation du plomb sur monozircon remet en question l'existence d'un socle Précambrien. – *C. R. Acad. Sci*., Paris, **320**, 1179-1185.

DELAPERRIERE E. & SOLIVA J. (1992). – Détermination d'un âge Ordovicien supérieur – Silurien pour les gneiss de Casemi (massif du Canigou, Pyrénées orientales) par la méthode d'évaporation du plomb sur monozircon. – *C. R. Acad. Sci.,* Paris, **314**, 345-350.

DELOULE E., ALEXANDROV P., CHEILLETZ A., LAUMONIER B. & BARBEY P. (2002). – In situ U-Pb zircon ages for early Ordovician magmatism in the eastern Pyrénées, France: the Canigou orthogneiss. – *Int. J. Earth Sci*. (*Geol. Rundsch*.), **91**, 398-405.

DEMANGE M. (1998). – Contribution au problème de la formation des dômes de la zone axiale de la Montagne-Noire. – *Géol. France*, **4**, 3-56.

DEMANGE M.(2003). – Formations du domaine varisque, 34-41. *In*: B. ALABOUVETTE, M. DEMANGE, J. GUERANGE-LOZES & P. AMBERT (Eds), Notice explicative carte géologique de la France à 1/250 000. Feuille Montpellier N° 38. – BRGM– Orléans.

GEBAUER D., WILLIAMS I.S., COMPSTON W. & GRÜNENFELDER M. (1989). – The development of the Central European continental crust since early Archean by ion-probe dating of old detrital zircons. – *Tectonophysics*, **157**, 81-96.

GIL IBARGUCHI J.I., NAVIDAD M. & ORTEGA L. (1990). – Ordovician and Silurian igneous rocks and orthogneiss in Catalonian Coastal Ranges. – *Acta Geol. Hispanica*. **25**, 29-90.

GRADSTEIN F.M. & OGG A.G. (2004). – International stratigraphic chart. – International Commission of Stratigraphy.

GRAY R.D., HAND M., MAWBY J., ARMSTRONG R.A., MCL. MILLER J. & GREGORY R.T. (2004). – Sm-Nd and zircon U-Pb ages from garnet-bearing eclogites, NE Oman: constraints on high-P metamorphism. – *Earth Planet. Sci. Lett*., **222**, 407-422.

GUITARD G. (1970). – Le métamorphisme hercynien mésozonal et les gneiss oeillés du massif du Canigou (Pyrénées orientales). – *Mém. du BRGM*, **63,** Eds BRGM Orléans.

GUITARD G., AUTRAN A. & FONTEILLES M. (1996). – Le substratum précambrien du Paléozoïque. *In*: A. BARNOLAS & J.-C. CHIRON, Eds. Synthèse géologique et géophysique des Pyrénées. Tome 1 – Cycle Hercynien. – BRGM –ITGE, Orléans & Madrid. 137-155.

JÄGER E. & ZWART H.J. (1968). – Rb-Sr age determinations of some gneisses and granites of the Aston-Hospitalet massif (Pyrenees). – *Geol. Mijnb.*, **47**, 349-357.

KONZALOVA M., CASAS J.M., FONTBOTE J.M. & SANTANACH P. (1982). – Nouvelles données micropaléontologiques sur le Paléozoïque inférieur de la zone axiale des Pyrénées catalanes. – *C. R. Acad. Sci.,* Paris, **294,** (II), 869-874.

KROGH T.E. (1973). – A low-contamination method for hydrothermal decomposition of zircon and extraction of U and Pb for isotopic age determination. – *Geochim. Cosmochim. Acta*, **37**, 485-494.

KROGH T.E. (1982a). – Improved accuracy of U-Pb zircon dating by selection of more concordant fractions using a high gradient magnetic separation technique. – *Geochim. Cosmochim. Acta*, **46**, 631-635.

KROGH T.E. (1982b). – Improved accuracy of U-Pb zircon ages by creation of more concordant systems using an air abrasion technique. – *Geochim. Cosmochim. Acta*, **46**, 637-649.

LAUMONIER B. (1988). – Les groupes de Canaveilles et de Jujols (« Paléozoïque inférieur ») des Pyrénées orientales. – *Hercynica*, **1**, 25-38.

LAUMONIER B. (1998). – Les Pyrénées centrales et orientales au début du Paléozoïque (Cambrien *s.l.*): évolution paléogéographique et géodynamique. – *Geodin. Acta*, **11**,1-11.

LAUMONIER B. (coord.) *et al.* (1996). – Cambro-Ordovicien *In*: BARNOLAS et CHIRON Eds. Synthèse géologique et géophysique des Pyrénées. Tome 1. Cycle hercynien. – BRGM-ITGE Orléans-Madrid,157-209.

LAUMONIER B. & GUITARD G. (1986). – Le Paléozoïque inférieur de la moitié orientale de la Zone Axiale des Pyrénées. Essai de synthèse. – *C. R. Acad. Sci*., Paris, **302**, 473-478.

LAUMONIER B., AUTRAN A., BARBEY P., CHEILLETZ A., BAUDIN T., COCHERIE A. & GUERROT C. (2004). – Le Précambrien du sud de la France (Pyrénées, Montagne Noire): mise au point, comparaison avec l'Ibérie centrale. – *Bull. Soc. géol. Fr.*, **175**, 6, 643-655.

LESCUYER J.-L. & COCHERIE A. (1992). – Datation sur monozircons des métadacites de Sériès: arguments pour un âge protérozoïque terminal des « schistes X » de la Montagne Noire (Massif central français). – *C. R. Acad. Sci.,* Paris, **314**, 1071-1077.

LUDWIG K.R. (2000). – Users manual for ISOPLOT/EX, version 2. A geochronological toolkit for Microsoft Excel. – Berkeley Geochronology Center, Special Publication 1a, 43 p.

MAJOOR F.J.M. (1988). – A geochronological study of the Axial zone of central Pyrénées, with emphasis on Variscan events and Alpine resetting. – Thesis, Univ. Amsterdam,-Verhand 6. Laborat. Isotop. Geology, 120 p.

NAVIDAD M. & CARRERAS J. (2002). – El volcanismo de la base del Paleozoico Inferior del macizo del Canigo (Pireneos Orientales). Evidencias geoquimicas de la apertura de una cuenca continental. – *Geogaceta*, **32**, 91-94.

NEUBAUER F. (2002) – Evolution of late Neoproterozoic to late early Paleozoic tectonic elements in Central and Southeast European Alpine Mountain belts: review and synthesis. – *Tectonophysics*, **352**, 87-103.

PACES J.B. & MILLER J.D. (1993). – Precise U-Pb ages of Duluth Complex and related mafic intrusions, northern Minnesota: geochronological insight to physical, petrogenic, and tectonomagmatic processes associated with the 1.1 Ga midcontinent rift system. – *J. Geophys. Res.*, **98**, 13997-14013.

PARRISH R.R. (1987). – An improved micro-capsule for zircon dissolution in U-Pb geochronology. – *Chem. Geol.* (Isotope Geoscience Section), **66**, 99-102.

PIN C. & MARINI F. (1993). – Early Ordovician continental break-up in Variscan Europe: Nd-Sr isotopes and trace elements; evidence from bimodal igneous associations of the southern Massif Central, France. – *Lithos*, **29**, 177-196.

PUPIN J.P. (1980). – Zircon and granite petrology. – *Contrib. Mineral. Petrol.,* **73**, 207-220.

ROGER F., RESPAUT J.-P., BRUNEL M., MATTE PH. & PAQUETTE J.-L. (2004). – Première datation U-Pb des orthogneiss œillés de la zone axiale de la Montagne noire (Sud du Massif central) : nouveaux témoins du magmatisme ordovician dans la chaîne varisque. – *C. R. Geoscience*, **336**, 19-28.

STACEY J.S. & KRAMERS J.D. (1975). – Approximation of terrestrial lead isotope evolution by a two-stage model. – *Earth Planet. Sci. Lett*., **26**, 207-221.

STAMPFLI G. M. (1996). – The Intra-Alpine terrane: a Paleotethyan remnant of the Alpine Variscides. – *Eclogae Geol. Helv.,* **89**, 13-42.

STAMPFLI G. M. & BOREL G. D. (2002). – A plate tectonic model for the Paleozoic and Mesozoic constrained by dynamic plate boundaries and restored synthetic oceanic isochrons. – *Earth Planet. Sci. Lett*., **196**, 17-33.

TERA F. & WASSERBURG G.J. (1972). – U-Th-Pb systematics in three Apollo 14 basalts and the problem of initial Pb in lunar rocks. – *Earth Planet. Sci. Lett*., **14**, 281-304.

VON RAUMER J.F., STAMPFLI G.M. & BUSSY F. (2003). – Gondwana-derived microcontinents – the constituents of the Variscan and Alpine collisional orogens. – *Tectonophysics,* **365**, 7-22.

VITRAC-MICHARD A. & ALLEGRE C.J. (1975a). – Study of the formation and history of a piece of continental crust by ^{87}Rb-^{86}Sr method: the case of the French Oriental Pyrenees. – *Contrib. Mineral. Petrol*., **50**, 257-285.

VITRAC-MICHARD A. & ALLEGRE C.J. (1975b). – ^{238}U-^{206}Pb, ^{235}U-^{207}Pb systematics on Pyrenean basement. – *Contrib. Mineral. Petrol*., **51**, 205-212.

WENDT I. & CARL C. (1991). – The statistical distribution of the mean squared weighted deviation. – *Chem. Geol*., **86**, 275-285.

WILLLIAMS I.S. (1998). – U-Th-Pb geochronology by ion microprobe. – *Rev. Eco. Geol*., **7**, 1-35.

WILLLIAMS I.S. (2001). – Response of detrital zircon and monazite, and their U-Pb isotopic systems, to regional metamorphism and host-rock partial melting, Cooma Complex, southeastern Australia. – *Aus. J. Earth Sci*., **48**, 557-580.